Catal Lett (2009) 131:328–336
DOI 10.1007/s10562-009-9945-7

Controlled Hydrogenation of Acetophenone Over Pt/CeO_2–MO_x (M = Si, Ti, Al, and Zr) Catalysts

Benjaram M. Reddy · Komateedi N. Rao · Gunugunuri K. Reddy

Received: 29 January 2009 / Accepted: 16 March 2009 / Published online: 27 March 2009

Abstract Vapour phase selective hydrogenation of acetophenone has been performed over a series of Pt/CeO_2–MO_x (MO_x = SiO_2, Al_2O_3, TiO_2, and ZrO_2) catalysts. The controlled hydrogenation was carried out in the 453–533 K temperature range at normal atmospheric pressure. The ceria-based mixed oxides were prepared through a co-precipitation or deposition-precipitation route. Platinum was deposited by a wet impregnation method. The obtained catalysts were calcined at 773 K and characterized by means of X-ray diffraction, Raman spectroscopy, BET surface area, temperature programmed reduction, temperature programmed desorption, thermogravimetry, and scanning electron microscopy. XRD analyses suggest that CeO_2–SiO_2 and CeO_2–Al_2O_3 primarily consist of CeO_2 nanoparticles dispersed over the amorphous silica or alumina surface. In the case of CeO_2–TiO_2, presence of segregated nanocrystalline CeO_2 and TiO_2-anatase phase were noted. Formation of cubic $Ce_{0.75}Zr_{0.25}O_2$ solid solution was observed in the case of CeO_2–ZrO_2. No peaks pertaining to platinum could be detected from XRD profiles. Formation of zirconia rich tetragonal phase ($Ce_{0.4}Zr_{0.6}O_2$) was observed in the case of Pt/CeO_2–ZrO_2 sample. Raman measurements revealed the fluorite structure of ceria and presence of oxygen vacancies in all samples. TPR results suggest that the presence of Pt facilitates the reduction of ceria. The catalytic performance of Pt-based catalysts was found to depend strongly on the nature of the support oxide employed. Among various catalysts investigated, the Pt/CeO_2–SiO_2 catalyst exhibited better product yields.

B. M. Reddy (✉) · K. N. Rao · G. K. Reddy
Inorganic and Physical Chemistry Division, Indian Institute of Chemical Technology, Uppal Road, Hyderabad 500607, India
e-mail: bmreddy@iict.res.in; mreddyb@yahoo.com

Keywords Supported platinum catalysts · Selective hydrogenation · Acetophenone · Phenyl ethanol · Effect of support · CeO_2-based mixed oxides · Catalyst characterization

1 Introduction

The catalytic hydrogenation of organic derivatives containing a carbonyl group is an important reaction widely used in the preparation of intermediates for fine chemicals and pharmaceuticals. The selective hydrogenation of a molecule containing both C=C and C=O bonds possesses commercial importance and has been investigated intensively [1–5]. However, the other interesting aspect of competitive hydrogenation between phenyl and carbonyl groups within a molecule has not been significantly discussed in previous publications so far. The hydrogenation of acetophenone is particularly important because of the enormous industrial use of two of the possible products: 1-phenyl ethanol (PE) and 1-cyclohexyl ethanol (CHE). In fact, CHE is employed in the manufacturing of various polymers, while PE finds use in the pharmaceutical and perfumery industries [6–8].

Conventional reduction processes employ inorganic hydrides ($LiAlH_4$ and $NaBH_4$) as reducing agents and produce a considerable amount of toxic residues, something unacceptable on the industrial scale from the environmental point of view. Heterogeneous catalytic hydrogenation offers the possibility to recover the catalyst and to use it again, thus minimizing the production of undesirable residues. These features make it a highly viable enviro-economic option for the reduction of aromatic ketones. In general, the reaction is carried out at low

hydrogen pressures and in the presence of supported metallic catalysts based on transition metals. Hence many by-products are formed during the course of the hydrogenation; achieving high selectivity towards a desired product is the major goal. However, use of monometallic platinum with hydrogen gas leads to the formation of phenyl ring hydrogenated product. Therefore, one needs to modify hydrogenating ability of Pt by promoting with another metal or supporting over a suitable carrier to improve selectivity towards alcohol. The promotion could involve either C=O double bond polarization and/or inhibition of phenyl ring adsorption through C=C bond. This promotion can be achieved by the addition of second, more electropositive metal like iron [9] or tin [10, 11] or by the use of supports such as CeO_2 [12–15], TiO_2 [16, 17], ZnO_2 [18], MgO [19] or SnO_2 [20], which are able to interact with platinum.

Support plays an important role in the catalytic activity and product selectivity of precious metals. In fact the metallic sites, usually active for hydrogenation of phenyl ring, are transformed into polar sites to activate the carbonyl group by interacting with the support. Cerium oxide is one of best applied promoters in heterogeneous catalytic reactions, mainly due to its critical role in the performance of three-way catalysts for automotive exhaust gas treatment and other applications [21]. The existence of metal-support interaction in CeO_2-promoted noble metal catalysts can be assessed not only by following the inhibition of H_2 or CO chemisorption ability of the catalyst when the reduction temperature is increased, but also with the help of probe reactions such as hydrogenation, for which both the activity and the selectivity are generally dependent on the reduction temperature. However, it has been reported that addition of CeO_2 to Ru and Co enhances production of long chain hydrocarbons and alkenes [22]. In all cases, effect of ceria seems to be related to the activation of C=O bond through the interaction of oxygen atom with oxygen vacancies, which are created at the ceria surface up on the reduction treatment. It was also reported that Pt catalysts prepared from chloride precursors are more selective towards hydrogenation of C=O than analogous catalysts prepared from tetramine platinum nitrate [13, 18, 23]. So far several reports have appeared on the liquid phase hydrogenation of acetophenone under different reaction conditions. Studies on the gas phase hydrogenation of acetophenone with well-defined metal surfaces are scarce in the literature. Therefore, the present systematic investigation was undertaken to resolve some of the aforesaid issues.

In the present study, a series of Pt supported CeO_2 and CeO_2–MO_x (MO_x = SiO_2, Al_2O_3, TiO_2, and ZrO_2) catalysts were prepared by precipitation and impregnation methods and characterized by using TGA, BET-SA, XRD, Raman, TPR, TPD, and SEM techniques. The synthesized catalysts were evaluated for hydrogenation of acetophenone in vapor phase at normal atmospheric pressure. For the purpose of better understanding, characterization results pertaining to pure ceria-based supports are also presented in this manuscript.

2 Experimental

2.1 Catalyst Preparation

The CeO_2–SiO_2 and CeO_2–Al_2O_3 mixed oxides were prepared by a deposition precipitation method, whereas CeO_2, CeO_2–TiO_2 and CeO_2–ZrO_2 mixed oxides (1:1 mole ratio based on oxides) were prepared by a precipitation or coprecipitation method. More detailed description of various preparative steps involved during the synthesis can be found elsewhere [24]. The platinum loaded catalysts were prepared by a standard wet impregnation method. To impregnate Pt (1 wt%), the requisite quantity of H_2PtCl_4 (SD fine chem., AR Grade) was dissolved in distilled water. To this clear solution, the finely powdered (773 K calcined) supports were added. The excess water was evaporated on a water bath under constant mechanical agitation. The obtained materials were washed thoroughly with hot water until free from chloride impurities, subsequently dried at 373 K for 10 h and calcined at 773 K for 5 h in a closed muffle furnace.

2.2 Catalyst Characterization

The DTA–TGA curves were obtained on a Mettler Toledo TG-SDTA apparatus. Sample (ca. 12 mg) was heated from ambient to 1,173 K under nitrogen flow and the heating rate was 10 K/min. Specific surface areas were determined by N_2 physisorption at liquid-N_2 temperature on a Micromeritics Gemini 2360 instrument. Prior to measurements, samples were oven dried at 393 K for 12 h and flushed with Ar gas for 2 h. X-ray powder diffraction patterns were recorded on a Rigaku Miniflex diffractometer, using Ni-filtered Cu Kα (0.15418 nm) radiation source. The average crystallite size of ceria was estimated with the help of Debye–Scherrer equation, using the XRD data of all prominent lines [25]. The Raman spectra were recorded on a HORIBA JOBIN YVON HR 800 spectrometer at ambient temperature. The emission line at 632.81 nm from an Ar+ ion laser (Spectra Physics) was focused, on the sample under the microscope. Temperature programmed reduction measurements were carried out on a Micromeritics Auto Chem 2910 instrument with TCD detector. The sample was treated with flowing He at 403 K for 90 min before the run. The experiments were performed using 5% H_2/Ar gas flow of 30 mL/min and about 100 mg of sample,

with a heating rate of 10 K/min. SEM analyses were carried out with a Jeol JSM 5410 microscope, operating with an accelerating voltage of 15 kV. Temperature programmed desorption measurements were performed using 100 mg of catalyst after pretreatment at 573 K under a dry He flow (50 mL/min). The catalyst was exposed to 10% NH_3 in He for 45 min at 373 K and excess NH_3 was removed under He flow. The temperature of the sample was raised at a rate of 10 K/min up to 1,073 K and a TCD detector monitored the desorbed gas.

2.3 Catalyst Evaluation

Hydrogenation of acetophenone was carried out in a down flow vertical fixed bed differential quartz micro-reactor (i.d. 10 mm, length 25 cm) at normal atmospheric pressure. In a typical experiment, ca. 200 mg of sieved catalyst with twice the amount of quartz particles was secured between two plugs of quartz wool. Ceramic beads were filled above the catalyst bed for better mixing of the reactants. Temperature of the reactor was monitored by a thermocouple with its tip located near the catalyst bed and connected to a temperature-indicator controller. Catalyst was pre-reduced in flowing 5% H_2 in N_2 (30 mL/min) at 673 K for 2 h. Acetophenone (Aldrich AR, Germany) was fed (1.5 mL/h) from a motorized syringe pump (Perfusor Secura FT, Germany) into the vaporizer where it was mixed uniformly with H_2 gas (60 mL/min). The liquid products collected through ice-cooled freezing traps were analyzed by a gas chromatograph using BP20-WAX capillary column and FID detector. The activity data were collected under steady-state conditions. The conversion, selectivity and yield were calculated as per the procedure described elsewhere [26].

3 Results and Discussion

The BET surface areas of Pt-impregnated samples and pure supports calcined at 773 K are shown in Table 1. All mixed oxide supports exhibited higher specific surface area than pure ceria. Mixed oxide supports prepared by deposition precipitation method exhibited higher surface areas than the samples obtained by co-precipitation method. Among various mixed oxide supports, ceria-silica exhibited highest specific surface area (203 m^2/g) as expected. Silica is well-known stabilizing agent for CeO_2 and the use of colloidal silica dispersion during the preparation leads to the formation of a high SA materials. The CeO_2–Al_2O_3 mixed oxide also exhibited reasonably a specific surface area (132 m^2/g) which is also obtained by deposition precipitation route. A slight decrease in the surface areas were observed after impregnation with platinum. This is mainly due to the penetration of the dispersed Pt into the pores of the support thereby narrowing its pore diameter and blocking some of the micropores [26–28].

Table 1 BET surface area, crystallite size measurements and cell parameter values of CeO_2 in Pt/CeO_2–MO_x (MO_x = SiO_2, Al_2O_3, TiO_2, and ZrO_2) samples calcined at 773 K (C-CeO_2, CS-CeO_2–SiO_2, CA-CeO_2–Al_2O_3, CT-CeO_2–TiO_2, CZ-CeO_2–ZrO_2, PC-Pt/CeO_2, PCS-Pt/CeO_2–SiO_2, PCA-Pt/CeO_2–Al_2O_3, PCT-Pt/CeO_2–TiO_2, and PCZ-Pt/CeO_2–ZrO_2)

Sample	Surface area (m^2/g)	Crystallite size (nm)	Cell parameter (Å)
C	57	12	5.40
PC	42	12.4	ND
CS	203	3.2	5.40
PCS	174	3.6	ND
CA	158	3.7	5.40
PCA	104	3.9	ND
CT	95	10.0	5.38
PCT	67	10.5	ND
CZ	84	4.7	5.35
PCZ	62	4.9	ND

ND not determined due to compositional heterogeneity and peak broadness

Figures 1 and 2 show the XRD patterns of various mixed oxide supports and Pt impregnated samples. In general, the XRD patterns of Pt-impregnated samples are broader than that of the pure supports. Pure ceria exhibited prominent diffraction lines characteristic of cubic fluorite structure of ceria. In the case of ceria-alumina, only broad diffraction lines due to ceria could be noted, while peaks

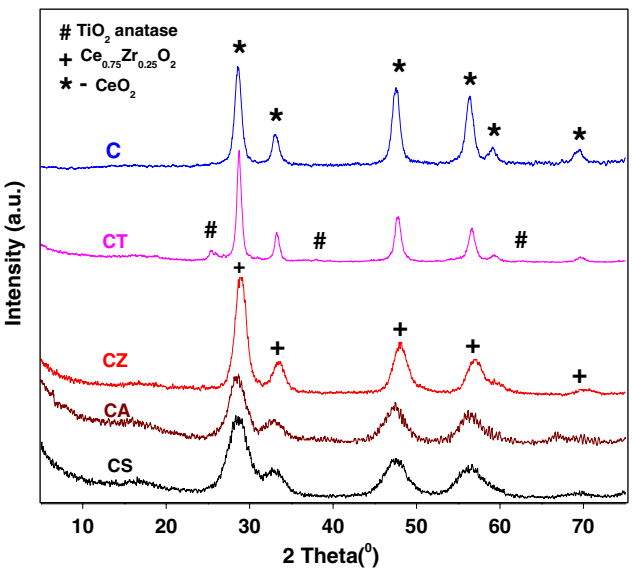

Fig. 1 X-ray powder diffraction patterns of CeO_2–MO_x samples (C-CeO_2, CS-CeO_2–SiO_2, CA-CeO_2–Al_2O_3, CT-CeO_2–TiO_2, and CZ-CeO_2–ZrO_2)

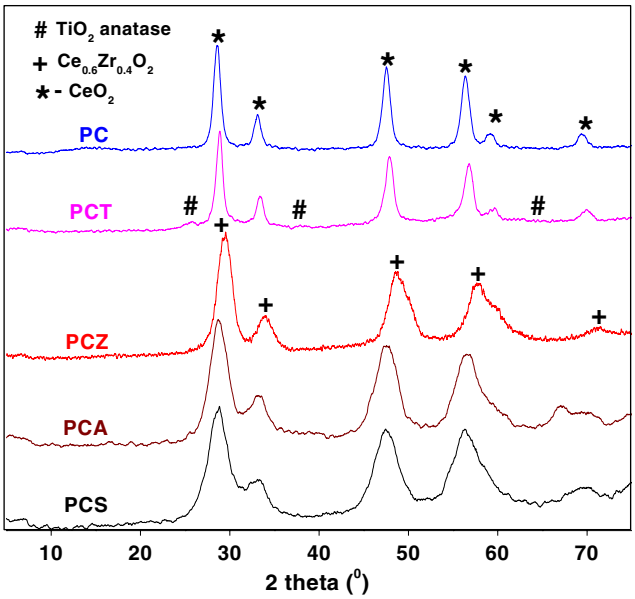

Fig. 2 X-ray powder diffraction patterns of $Pt/CeO_2–MO_x$ samples (PC-Pt/CeO_2, PCS-$Pt/CeO_2–SiO_2$, PCA-$Pt/CeO_2–Al_2O_3$, PCT-$Pt/CeO_2–TiO_2$, and PCZ-$Pt/CeO_2–ZrO_2$)

pertaining to Al_2O_3 were not detected. Similarly, $CeO_2–SiO_2$ support exhibited poor crystallinity and the diffraction lines due to CeO_2 were observed. The non-appearance of SiO_2 diffraction patterns indicates that silica is in highly amorphous state. Another observation to be noted from XRD measurements is that there are no lines due to compounds or mixed phases of ceria and silica. Recently, Rocchini et al. [29, 30] reported the formation of $Ce_{9.33}(SiO_4)_6O_2$ phase in their investigation where a different preparation method and a high calcination temperature was employed. Separate peaks due to CeO_2 and TiO_2 (A) phases were noted in $CeO_2–TiO_2$ sample, while the formation of a solid solution of specific composition $Ce_{0.75}Zr_{0.25}O_2$ is observed in the case of ceria-zirconia support. In the Pt loaded samples, there were no specific XRD peaks due to platinum or related compounds. Formation of alloy between Pt and CeO_2 is well documented in the literature [31–34]. Pt and ceria are known to mix in various stoichiometric compositions. Five well-known Pt–Ce intermetallic compounds: CePt, $CePt_2$, Ce_3Pt_2, Ce_7Pt_3, and $CePt_5$ were also documented in the literature [31–34]. The formation of $CePt_5$ phase has also been proposed to be responsible for the deactivation of Pt/CeO_2 catalyst reduced at 773 K [13, 35]. The present results give an impression that Pt slightly accelerates the crystallization of ceria. The impregnated Pt on $CeO_2–ZrO_2$ also facilitates slight zirconium enrichment, as evidenced by the existence of $Ce_{0.4}Zr_{0.6}O_2$ phase. Generally, the loss of catalytic activity of Pt/CeO_2 is attributed to the formation of alloys. Interestingly, there is no such alloy formation in the present investigation. The results commanded here suggest it is very unlikely that the occurrence of alloying phenomena after reduction at such a relatively moderate temperature.

Crystallite sizes (D_{XRD}) of CeO_2 or $Ce_{1-x}Zr_xO_2$ in $CeO_2–MO_x$ and $Pt/CeO_2–MO_x$ ($MO_x = SiO_2$, Al_2O_3, TiO_2, and ZrO_2) samples calcined at 773 K are summarized in Table 1. The mixed oxide supports prepared by deposition precipitation method yielded much smaller crystallites than the samples obtained by co-precipitation route. The precipitation of mixed oxides from cerium ammonium nitrate along with colloidal silica or alumina could yield smaller crystallites of ceria on the surface of silica or alumina. The deposition-precipitation technique takes the advantage of the fact that precipitation onto the carrier needs a lower super saturation than formation of new phases directly from the liquid (co-precipitation route). When compared to platinum free supports, the crystallite size of Pt-containing catalysts is larger, which indicates that the impregnated Pt accelerates the grain growth. Thus, it can be inferred from Table 1 that the crystallization depends on the presence of dispersed Pt. Interestingly, the XRD measurements of $Pt/CeO_2–ZO_2$ sample indicated that impregnated platinum not only accelerates the grain growth of ceria-zirconia solid solution but also induces more incorporation of zirconium into the ceria cubic lattice, leading to the formation of zirconium-rich tetragonal phase [24].

Raman spectra of various support oxides are collected in Fig. 3. As presented in Fig. 3, all samples show a prominent peak at around 457–470 cm^{-1} and a weak band at 600 cm^{-1}. The band at 457 cm^{-1} corresponds to the triply

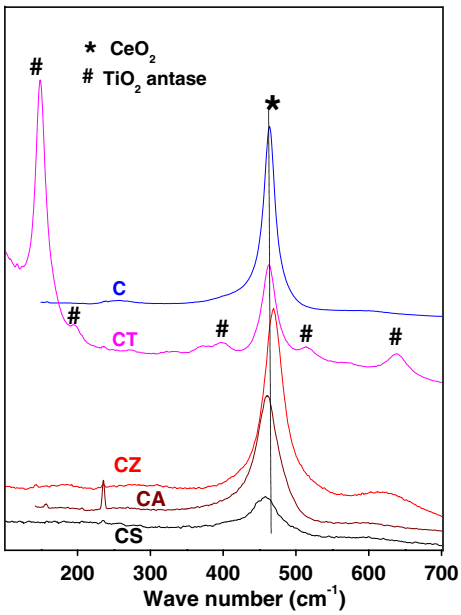

Fig. 3 Raman spectra of $CeO_2–MO_x$ samples (C-CeO_2, CS-$CeO_2–SiO_2$, CA-$CeO_2–Al_2O_3$, CT-$CeO_2–TiO_2$, and CZ-$CeO_2–ZrO_2$)

degenerate F_{2g} mode and can be viewed as a symmetric breathing mode of oxygen atoms around the cerium ions [36]. The weak band observed at around 600 cm^{-1} could be assigned to a non-degenerate LO mode of CeO_2 [36–39]. Both CeO_2–Al_2O_3 and CeO_2–SiO_2 mixed oxides exhibited similar Raman bands. Furthermore, silica and alumina did not show any Raman features, as reported in the literature [40]. This indicates that silica and alumina form part of the substrate support on which cerium oxide has been forming a surface over layer. The Raman spectrum of the CeO_2–TiO_2 sample revealed typical spectra of TiO_2 anatase and CeO_2 [36]. The Raman spectrum of CeO_2–ZrO_2 sample is dominated by a strong band at 470 cm^{-1} and a less prominent broad band at ~600 cm^{-1}. The small shift in the Raman frequency to higher wave numbers could be due to the incorporation of zirconium cations into the ceria lattice, as evidenced by XRD results. Thus, the Raman results corroborate well with the XRD observations. The Raman spectra of Pt impregnated samples (not shown) are similar to pure oxides and all the samples showed a prominent peak at 457–470 cm^{-1} and a weak band at ~600 cm^{-1}. There are no peaks pertaining to either Pt or compounds between Pt and ceria.

The reduction characteristics of various samples were investigated by TPR. The hydrogen consumption profiles obtained as a function of temperature are plotted in Fig. 4a. The TPR profile of pure CeO_2 is characterized by two reduction peaks. The peak at ~800 K could be assigned to the reduction of more super facial Ce^{4+}. The second peak observed at about 1,000 K, originates from the bulk reduction of the oxide. As observed from Fig. 4a, the SiO_2, Al_2O_3, and TiO_2-based oxides exhibit mostly similar TPR profiles. Primarily, the three mixed oxides show two broad reduction peaks, one at 730–780 K and the other at 800–900 K. The low temperature reduction peak is attributed to the reduction of surface-capping oxygen of ceria and the second high temperature peak is due to the bulk reduction. The TPR results are in agreement with the previous reports [12, 41–43]. The TPR profile of CeO_2–ZrO_2 mixed oxide is slightly different from the remaining three profiles. The easier reduction of CeO_2–ZrO_2 mixed oxide when compared to pure CeO_2 has been reported by several authors [44, 45]. It is mainly due to structural modification of ceria when some Ce^{4+} cations are substituted with smaller Zr^{4+} cations; thereby favouring the diffusion of O^{2-} anions within the lattice.

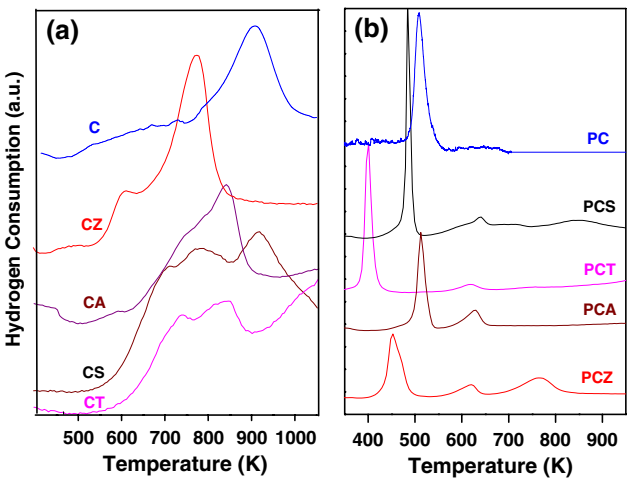

Fig. 4 TPR curves (H_2 consumption) for CeO_2–MO_x and Pt/CeO_2–MO_x samples (C-CeO_2, CS-CeO_2–SiO_2, CA-CeO_2–Al_2O_3, CT-CeO_2–TiO_2 and CZ-CeO_2–ZrO_2; PC-Pt/CeO_2, PCS-Pt/CeO_2–SiO_2, PCA-Pt/CeO_2–Al_2O_3, PCT-Pt/CeO_2–TiO_2, and PCZ-Pt/CeO_2–ZrO_2)

The incorporation of Pt to CeO_2–MO_x completely modified the TPR profiles as shown in Fig. 4b. Now the surface reduction peak in the region 750–800 K is completely lacking, giving rise to two new low temperature peaks in the range from 450 to 500 K and 600 to 650 K. The first one, centered in the low temperature region, is assigned to the surface reduction of CeO_2 in close contact with the metal as well as break down of Pt-O-Ce species. The second peak at about 620 K corresponds to the surface reduction of the ceria, which is not so close to platinum. Therefore, it can be stated that the presence of Pt clearly promotes the reduction of ceria, as evidenced by a shift in the TPR profiles of pure support (700–800 K) and Pt-impregnated samples (~500 K). The phenomenon is assigned to the ability of the noble metal to promote the reduction of ceria via spilling of hydrogen species over the support. The consumption of hydrogen is more in first peak when compared to second peak. This gives an impression that most of the ceria is in contact with platinum. Recently, Corma et al. [46] reported that Pt over ceria-silica exhibits a reduction peak at 367 K due to the reduction of noble metal particles that are not submitted to the strong-metal support interaction, i.e., Pt particles that are present over the silica. In the present investigation no such peaks are observed. This means that platinum is only in contact with ceria not with other components present in the support. These two are encouraging aspects of the present investigation. In conclusion, it seems clear from these results that in all cerium-containing catalysts, the reduction treatment at 673 K is sufficient to produce the surface reduction of ceria, with the creation of oxygen vacancies and the presence of Ce^{3+} ions. The temperature-programmed desorption of ammonia over the catalysts was carried out and the profiles are shown in Fig. 5. In general, silica-based catalyst shows more total acidity when compared to other catalysts. The more acidity in case of silica-based catalyst may be due to the presence of free silica. However, the acidity distribution is broad in all catalysts lying in the range of 473–873 K.

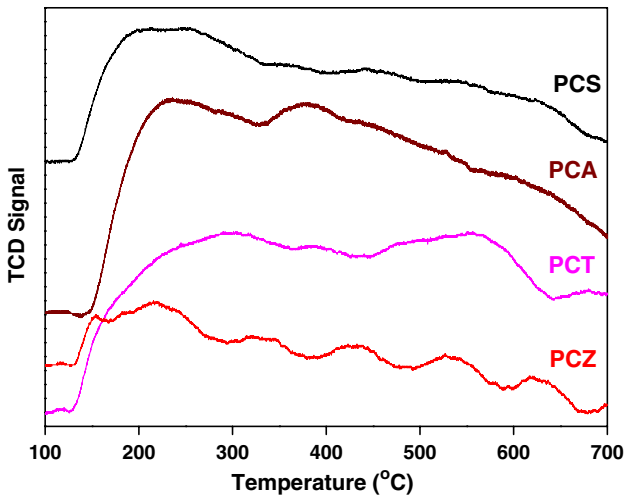

Fig. 5 TPD curves (NH_3 consumption) for Pt/CeO_2–MO_x samples (PCS-Pt/CeO_2–SiO_2, PCA-Pt/CeO_2–Al_2O_3, PCT-Pt/CeO_2–TiO_2, and PCZ-Pt/CeO_2–ZrO_2)

Figure 6 depicts the activity trend of various platinum-based catalysts as a function of time-on-steam. The activity of the catalysts without platinum i.e., on pure supports is negligible. However, Pt impregnated mixed oxide samples showed higher activity than the pure Pt/CeO_2 sample. This could be due to better dispersion of Pt over mixed oxides and better thermal stability of the supports. Among all the Pt supported catalysts, silica and alumina-based catalysts showed slightly higher activity compared to other two catalysts. This may be due to higher surface area and better dispersion of platinum over these supports. In the time-on-stream experiments, a slight decrease in activity was noted in the case of Pt/CeO_2–ZrO_2 and Pt/CeO_2–TiO_2 catalysts, while Pt/CeO_2–SiO_2 and Pt/CeO_2–Al_2O_3 exhibited stable activity. The main reason for deactivation of zirconia and titania supported catalysts is due to sintering of metal particles. These results can be explained from BET surface area values. Figure 7 shows the variation of selectivity with time-on-stream at a temperature of 453 K and flow rate of 1.5 mL/min on various Pt supported samples. All catalysts showed almost 100% selectivity towards phenylethanol and there is no decrease in the selectivity with time-on-stream. Figure 8 represents the SEM images of Pt impregnated CeO_2–SiO_2 and CeO_2–TiO_2 catalysts before and after the reaction. From the SEM images, considerable sintering can be observed in used ceria-zirconia supported catalyst.

The reaction was also carried out at different temperatures to study the effect of temperature on the conversion of acetophenone and selectivity of phenylethanol. The activity profiles obtained in the temperature range 453–533 K are displayed in Fig. 9. In general, in all cases an increase in the conversion with an increase of temperature was observed. All the catalysts except ceria-titania supported, exhibited 100% conversion at the highest temperature investigated. Although results of catalytic activity cannot be explained straightforward because of the conjunction of several factors; mainly due to the intrinsic activity of the catalyst and more or less pronounced deactivation. The

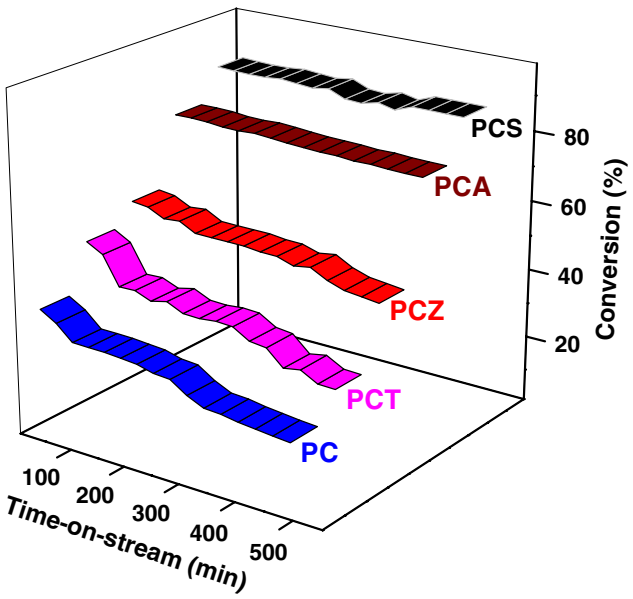

Fig. 6 Effect of time-on-stream on conversion of acetophenone over various Pt/CeO_2–MO_x catalysts at 453 K (PC-Pt/CeO_2, PCS-Pt/CeO_2–SiO_2, PCA-Pt/CeO_2–Al_2O_3, PCT-Pt/CeO_2–TiO_2, and PCZ-Pt/CeO_2–ZrO_2)

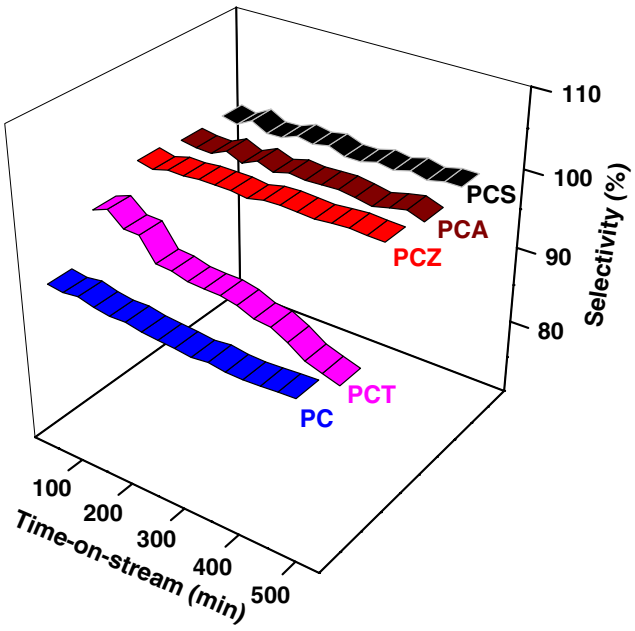

Fig. 7 Effect of time-on-stream on selectivity of phenyl ethanol over various Pt/CeO_2–MO_x catalysts at 453 K (PC-Pt/CeO_2, PCS-Pt/CeO_2–SiO_2, PCA-Pt/CeO_2–Al_2O_3, PCT-Pt/CeO_2–TiO_2, and PCZ-Pt/CeO_2–ZrO_2)

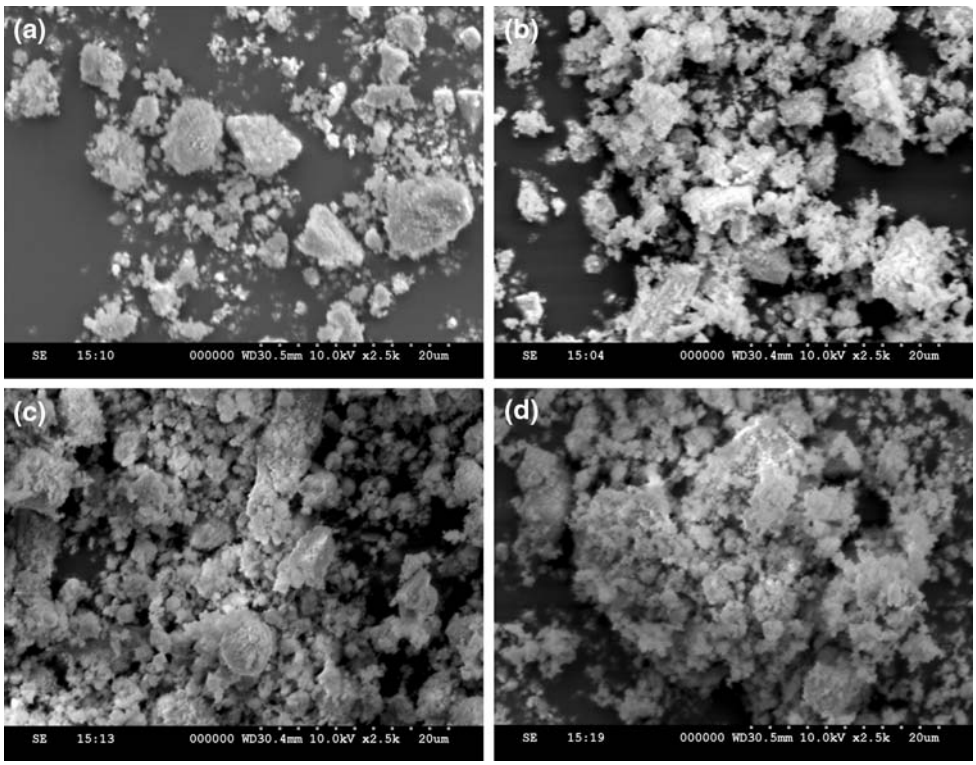

Fig. 8 SEM micrographs of catalysts before reaction **a** Pt/CeO_2–SiO_2, **b** Pt/CeO_2–ZrO_2; and after 500 min of reaction, **c** Pt/CeO_2–SiO_2, **d** Pt/CeO_2–ZrO_2

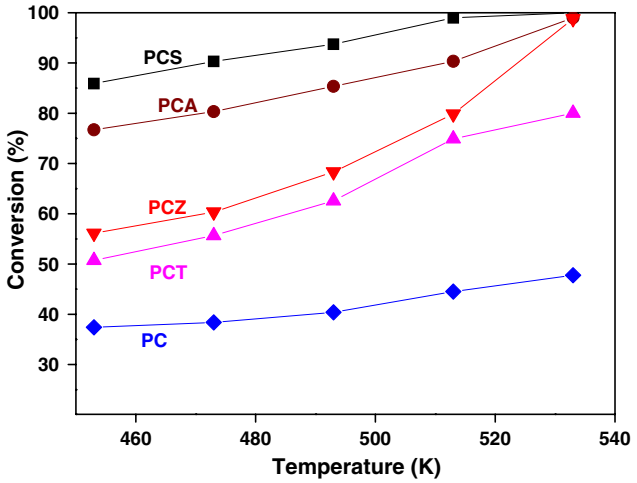

Fig. 9 Effect of temperature on conversion of acetophenone over various Pt/CeO_2–MO_x catalysts (PC-Pt/CeO_2, PCS-Pt/CeO_2–SiO_2, PCA-Pt/CeO_2–Al_2O_3, PCT-Pt/CeO_2–TiO_2, and PCZ-Pt/CeO_2–ZrO_2)

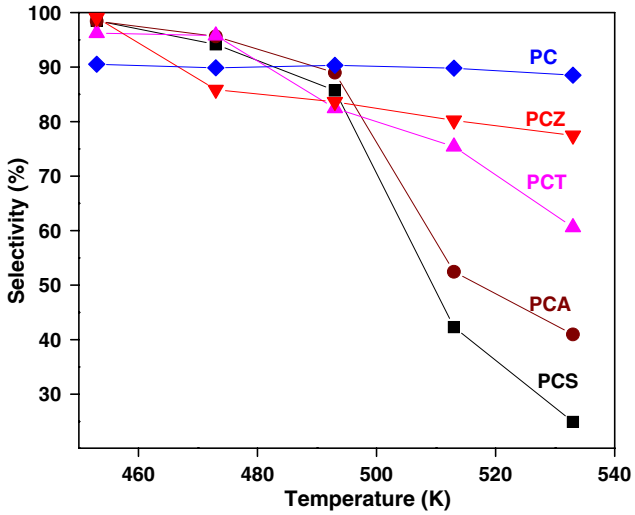

Fig. 10 Effect of temperature on selectivity of phenyl ethanol over various Pt/CeO_2–MO_x catalysts (PC-Pt/CeO_2, PCS-Pt/CeO_2–SiO_2, PCA-Pt/CeO_2–Al_2O_3, PCT-Pt/CeO_2–TiO_2, and PCZ-Pt/CeO_2–ZrO_2)

selectivity profiles as a function of temperature are presented in Fig. 10. The selectivity towards phenylethanol decreased with increasing reaction temperature and selectivity to ethyl benzene increased rapidly (not shown). The Pt/CeO_2–TO_2 catalyst showed a conversion of 50% at 453 K with 96% selectivity to phenylethanol. At 493 K the conversion increased to 62% and reaches 80% at 533 K, but at the same time the selectivity to phenylethanol decreased from 96 to 60% with the production of increasing amounts of ethylbenzene. The selectivity of ethylbenzene increased with increasing conversion, showing that it was a typical consecutive reaction in which phenyl ethanol was an intermediate in the process of ethylbenzene formation. Several authors have cited the consecutive reaction characteristics of acetophenone hydrogenation. Lenarda et al. [47] reported that the selectivity of phenylethanol decreases from 98 to 56% when the

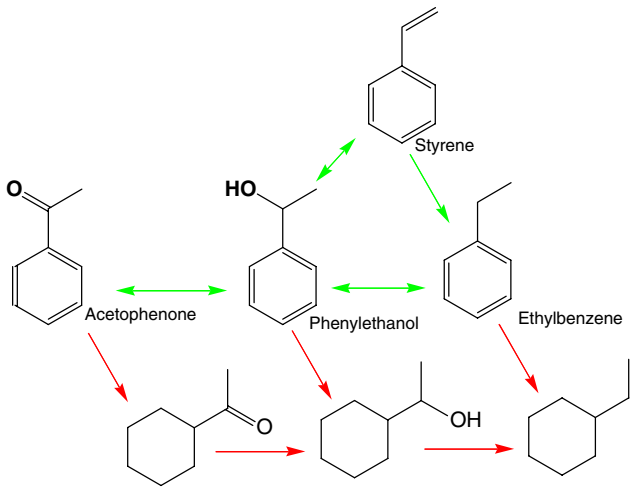

Scheme 1

conversion increases from 44 to 99% over Pd on Zn-Al hydrotalcite. The same authors also accounted that the selectivity of phenylethanol decreases from 60 to 0% and the selectivity of ethylbenzene increases from 40 to 91%, when the temperature increases from 333 to 423 K. Chen et al. [48] reported that the conversion of phenylethanol to ethylbenzene increases rapidly with the increase in conversion over reduced Pd/SiO_2 catalyst. The above studies confirm the rate of transformation of phenylethanol to ethylbenzene increase with increasing both conversion and temperature and the present results are inline with earlier reports. The decrease in the selectivity is more in case of ceria-silica and ceria-alumina samples. As per the proposed mechanism, the formation of ethylbenzene takes place in three steps, the first one being the hydrogenation of acetophenone over Pt sites leading to the formation of 1-phenyl ethanol, second being dehydration into styrene over acidic sites and finally which in turn get hydrogenated into ethylbenzene. The TPD results conclusively showed that surface acidity is more for silica and alumina based catalysts. Therefore, better activity and less selectivity (at higher reaction temperature) were observed over silica and alumina supported catalysts when compared to the titania and zirconia, as the former are more acidic (Scheme 1).

4 Conclusions

By adopting coprecipitation or deposition precipitation methodologies, a 1:1 molar ratio mixed oxides of CeO_2–MO_x ($MO_x = SiO_2$, Al_2O_3, TiO_2, and ZrO_2) were prepared. These preparations yielded fairly homogeneous and thermally stable mixed oxides with reasonably high specific surface areas. These oxides were used as supports for preparing platinum-based catalysts. XRD profiles of ceria-silica and ceria-alumina mixed oxides showed only peaks due to ceria. In case of CeO_2–ZrO_2 sample, formation of ceria-zirconia solid solution is observed. No platinum features were observed from either XRD or Raman measurements. XRD and Raman results conclude that Pt promotes the incorporation of more zirconium into the ceria lattice. TPR results suggest that presence of platinum promotes the reduction of ceria via hydrogen spillover. TPD results reveal that silica-based catalyst exhibits more acidity compared to other catalysts. Catalytic results indicate that the selectivity of phenyl ethanol depends on both temperature and conversion of acetophenone. Among the various catalysts investigated, Pt/CeO_2–SiO_2 sample showed better catalytic activity for acetophenone hydrogenation.

Acknowledgments KNR and GKR thank UGC, New Delhi for senior research fellowships.

References

1. Wismeijer AA, Kieboom APG, Van Bekkum H (1986) Appl Catal 25:181
2. Noller H, Lin WM (1984) J Catal 85:25
3. Hubaut R, Dage M, Bonnelle JP (1986) Appl Catal 22:231
4. Simonik J, Beranek P (1972) J Catal 24:348
5. Vannice MA, Sen B (1989) J Catal 115:65
6. Kashiwagi Y, Uchiyama K, Kurashima F, Kikuchi C, Anzai J (1999) Chem Pharm Bull 47:1051
7. Lavaud N, Magnoux P, Alvarez F, Melo L, Giannetto G, Guisnet M (1999) J Mol Catal A Chem 142:223
8. Rajashekharam MV, Bergault I, Foilloux P, Schweich D, Delmas H, Chaudari RV (1999) Catal Today 48:83
9. Marinelli TBLW, Nabuurs S, Ponec V (1995) J Catal 151:431
10. Coloma F, Escribano AS, Fierro JLG, Reinoso FR (1996) Appl Catal A Gen 148:63
11. Margitfalvi JV, Vanko G, Borbath I, Tompos A, Vertes A (2000) J Catal 190:474
12. Escribano AS, Coloma F, Reinoso FR (1998) J Catal 178:649
13. Abid M, Touroude R (2000) Catal Lett 69:139
14. Albero JS, Reinoso FR, Escribano AS (2002) J Catal 210:127
15. Escribano AS, Albero JS, Coloma F, Reinoso FR (2000) Stud Surf Sci Catal 130:1013
16. Dandekar A, Vannice MA (1999) J Catal 183:344
17. Vannice MA (1997) Top Catal 4:241
18. Consonni M, Jokic D, Murzin DY, Touroude R (1999) J Catal 188:165
19. Homs N, Llorca J, Ramirez de la Piscina P, Reinoso FR, Escribano AS, Albero JS (2001) Phys Chem Chem Phys 3:1782
20. Liberkova K, Touroude R (2002) J Mol Catal A Chem 180:221
21. Trovarelli A (1996) Catal Rev Sci Eng 38:439
22. Ruiz AG, Escribano AS, Ramos IR (1994) Appl Catal A Gen 120:71
23. Ammari F, Lamotte J, Touroude R (2004) J Catal 221:32
24. Reddy BM, Rao KN, Reddy GK, Khan A, Park SE (2007) J Phys Chem C 111:18758
25. Klug HP, LE Alexander (1974) X-ray diffraction procedures for polycrystalline and amorphous materials, 2nd edn. Wiley, New York

26. Reddy BM, Ganesh I, Khan A (2004) J Mol Catal A Chem 223:295
27. Reddy BM, Ganesh I, Reddy EP (1997) J Phys Chem B 101:1769
28. Reddy BM, Manohar B, Reddy EP (1993) Langmuir 9:1781
29. Rocchini E, Trovarelli A, Llorca J, Graham JW, Weber WH, Maciejewski M, Baiker A (2000) J Catal 194:461
30. Rocchini E, Vicario M, Llorca J, de Leitenburg C, Dolcetti G, Trovarelli A (2002) J Catal 211:407
31. Bronger W (1967) J Less Common Met 12:63
32. Le Roy J, Moreau JM, Paccard D (1978) Acta Cryst B 34:9
33. Compton VB, Matthias BT (1959) Acta Cryst 12:651
34. Dwight AE, Conner RA, Downey JW (1965) Acta Cryst 18:837
35. Meriaudeau P, Dutel JF, Dufaux M, Naccache C (1982) Stud Surf Sci Catal 11:95
36. Lin XM, Li LP, Li GS, Su WH (2001) Mater Chem Phys 69:236
37. Spanier SE, Robinson RD, Zhang F, Chan SW, Herman IP (2001) Phys Rev B 64:245407
38. Weber WH, Hass KC, McBride JR (1993) Phys Rev B 48:178
39. McBride JR, Hass KC, Poindexter BD, Weber WH (1994) J Appl Phys 76:2435
40. Wachs IE, Deo GJ (1991) J Phys Chem 95:5889
41. Yao HC, Yao YFY (1984) J Catal 86:54
42. de Leitenburg C, Trovarelli A, Kaspar J (1997) J Catal 166:98
43. Giordano F, Trovarelli A, de Leitenburg C, Giona M (2000) J Catal 193:273
44. Fornasiero P, Dimonte R, Rao GR, Kaspar J, Meriani S, Trovarelli A, Graziani M (1995) J Catal 151:168
45. Murota T, Hasegawa T, Aozasa S, Matsui H, Motoyama M (1993) J Alloys Compds 193:298
46. Corma A, Concepcion P, Albero JS, Franco V, Ching JYC (2004) J Am Chem Soc 26:5523
47. Lenarda M, Casagrande M, Moretti E, Storaro L, Frattini R (2007) Cat Lett 114:79
48. Chen CS, Chen HW (2004) Appl Catal A Gen 260:207